

Structure and Transport of the Antarctic Circumpolar Current at Drake Passage from Short-Term Measurements

WORTH D. NOWLIN, JR., AND THOMAS WHITWORTH III

Department of Oceanography, Texas A & M University, College Station 77843

R. DALE PILLSBURY

School of Oceanography, Oregon State University, Corvallis 97331

(Manuscript received 12 January 1977, in revised form 27 June 1977)

ABSTRACT

Three-week average speeds from an array of current meter moorings which spanned Drake Passage were used in conjunction with geostrophic calculations to estimate the short-term transport of the Antarctic Circumpolar Current. Closely spaced hydrographic stations show that the current consists of three vertically coherent bands of relatively high speed within the generally eastward flow. These bands separate four water mass regimes which have distinct *T-S* relationships at depths above the core of the Circumpolar Deep Water. The geostrophic transport relative to 3000 db averaged $95 \times 10^6 \text{ m}^3 \text{ s}^{-1}$ for five transects of the Passage and is consistent with previous measurements. Referencing the geostrophic transport to the current meter measurements gives an adjusted transport of $124 \times 10^6 \text{ m}^3 \text{ s}^{-1}$ to the east. This estimate is about midway between values obtained in the two previous attempts to adjust relative transport through Drake Passage to observed velocities. The previous estimates are reconsidered and compared with this latest estimate.

1. Introduction

The Southern Ocean is an important link in the world ocean, and it is important that its dynamics and general circulation be clearly understood. Knowledge of the transport of the Antarctic Circumpolar Current (ACC) and its variability will be useful in formulating the correct dynamical balance as well as aid in the development and testing of models of ocean circulation. Numerous estimates of the volume transport have been made, but because of the extreme width of the current and the difficulty in determining its northern boundary in the open ocean, most attempts have focused on the passage between Australia and Antarctica or on Drake Passage separating South America and Antarctica. The status of transport estimates through Drake Passage was summarized by Reid and Nowlin (1971). However, several other data sets are now available for comparison. This paper and the accompanying one by Bryden and Pillsbury (1977) examine the structure, transport and variability of the ACC at Drake Passage.

In 1975, oceanographers working as a part of the International Southern Ocean Studies (ISOS) began a long-term program aimed at studying the dynamics of the Antarctic Circumpolar Current. A central part of that program is to measure and describe the internal structure of the Current and to determine its trans-

port. As part of an initial field experiment, an array of instruments for measuring current, temperature and pressure was deployed across Drake Passage. Some of the current/temperature recorders were recovered after a period of approximately three weeks; the remainder was left for a period of approximately one year and then recovered. Several oceanographic sections spanning the Passage were made in support of the short-term current meter deployment.

The first purpose of this paper is to describe the structure of the water mass and current regimes and to present estimates of transport based on the results of this short-term experiment. The second purpose is to discuss the interpretations of other recent measurements and to compare our findings with those of other investigators. In the accompanying paper, Bryden and Pillsbury consider the year-long current records and estimate the variability of deep currents and of the associated referenced transport.

2. The FDRAKE measurements

The first ISOS experiment in the Antarctic Circumpolar Current was the 1975 First Dynamic Response and Kinematics Experiment (FDRAKE 75) conducted in January, February and March 1975. The three ships involved were the R/V *Melville* operated by the Scripps Institution of Oceanography, the R/V *Conrad*

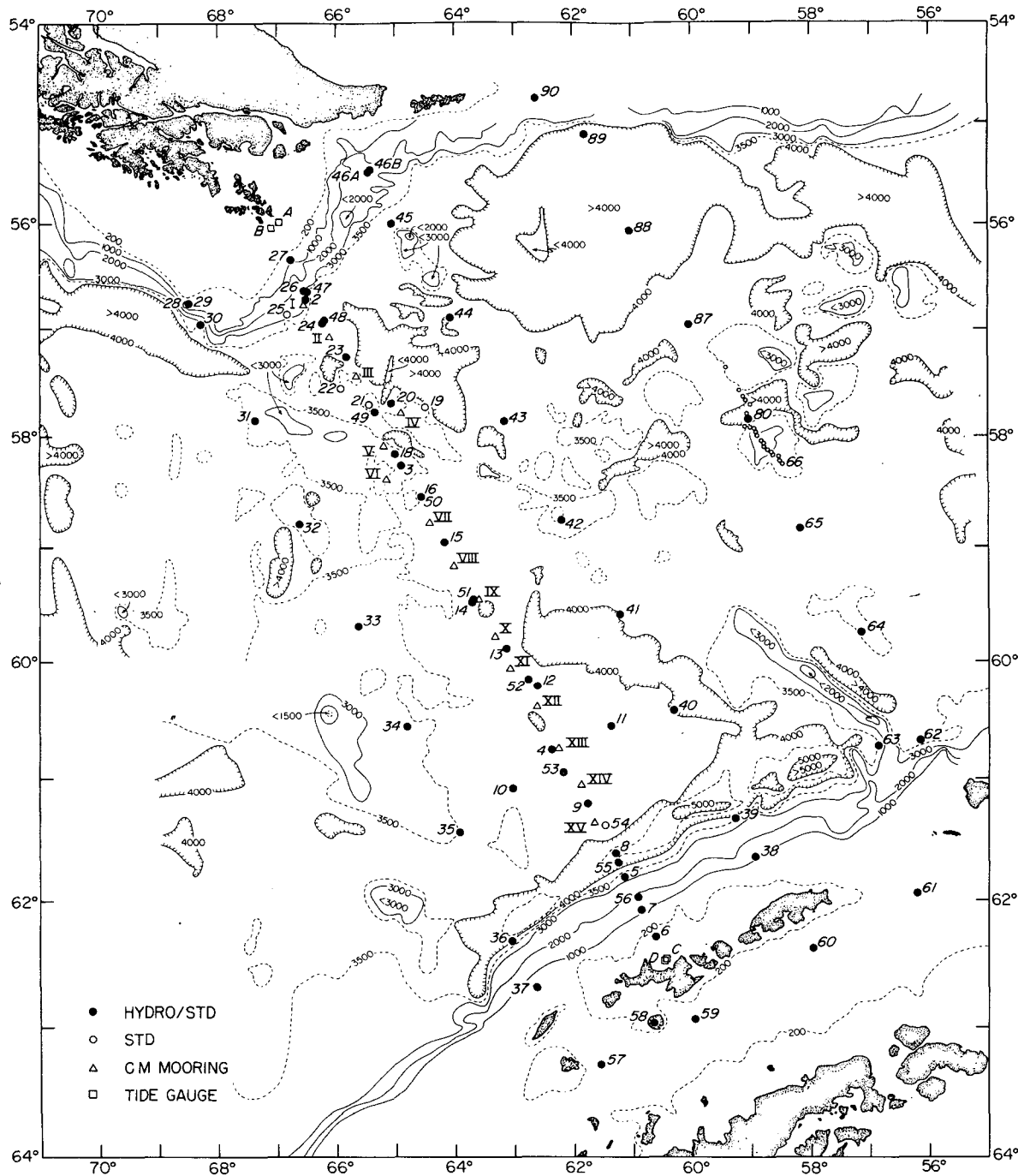


FIG. 1. Melville station plan, FDRAKE 75, 19 February-30 March 1975.

operated by the Lamont-Doherty Geological Observatory and the ARA *Islas Orcadas* operated by the Servicio de Hidrografia Naval of Argentina. Scientific results discussed in this paper are based on data collected aboard *Melville*.

During six crossings of Drake Passage, *Melville* deployed a current and temperature recording array, recovered the short-term component of that array

and made 90 hydrographic/STD stations. The station positions and current meter locations are shown in Fig. 1. Hydrographic sections II (Stations 7-27) and V (Stations 47-57) were made along the current meter line approximately three weeks apart. Two sections were made east of the current meter array (IV and VI) and one to the west (III). Nominal station separation was 55 km on section II and 110 km

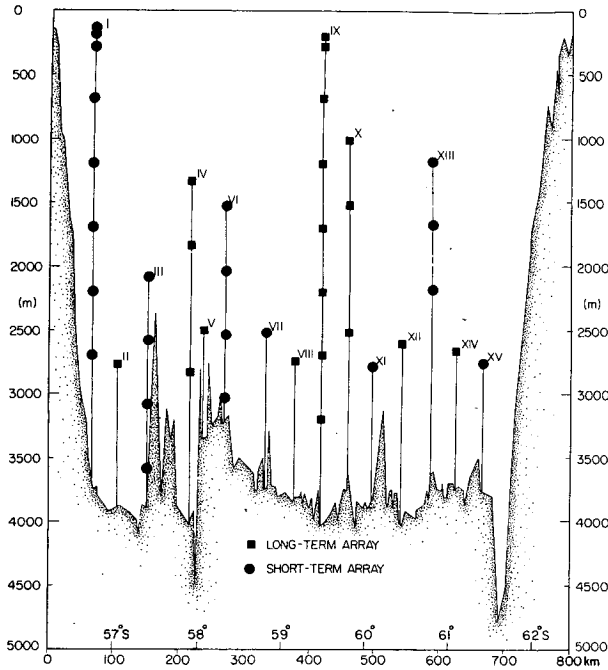


FIG. 2. FDRAKE 75 current meter array.

on other sections. The hydrographic stations in deep water consisted of a deep and a shallow cast, each with 7–22 Nansen bottles on the STD wire. The deep cast sampled as close as possible to the bottom. Data processing procedures and listings of hydrographic and STD measurements are given in Nowlin *et al.* (1977).

The current meter array is shown in Fig. 2. The entire array consisted of 16 General Oceanics model 2010 current meters and 27 Aanderaa RCM5 current meters deployed on 15 subsurface taut-wire moorings. An attempt was made to locate one meter on each mooring near 2700 m depth. All instruments internally recorded current speed and direction every hour; the Aanderaa meters also recorded temperatures hourly. Installation and recovery of the array was done by the current meter group at Oregon State University.

The short-term component of the array was recovered during hydrographic section V about three weeks after deployment. During FDRAKE 76 the remainder of the array was recovered by the R/V *Thompson* of the University of Washington and a new set of year-long moorings was deployed.

Fig. 3 shows the period of data return from each of the current meters. All equipment was recovered with the exception of the current meter on mooring V. Of the 24 meters in the short-term component of the array, only two returned with records of less than 20-day duration: the meter at 2700 m on mooring I failed after 6 days and the meter at 2530 m on mooring VI after 3 days. Of the 18 meters recovered from the year-long array, two of the Aanderaa meters (at 1340 and 1840 m on mooring IV) gave temperature

and direction only, the speed sensors having failed during installation. The General Oceanics meters on mooring IX yielded 14% data return with the longest record (5 months) at 1200 m containing the majority of the data.

The calibration and data processing procedures for the current meters are described in Pillsbury *et al.* (1974). Both pre- and post-calibrations were done on all Aanderaa instruments, and no significant differences were found. The General Oceanics meters gave erratic sample times and these data were interpolated to a uniform sample interval prior to analysis. The short-term data are described in detail by Pillsbury *et al.* (1976).

3. Water mass characteristics

Figs. 4a–4d show the vertical sections of temperature, salinity, dissolved-oxygen concentration and density for section II of *Melville*, FDRAKE 75. The bathymetry shown represents a composite of all the soundings made while working along the current meter array and is a projection of those soundings onto a straight line connecting Cape Horn with Desolation Island (located within the embayment Hero Bay, on the northern side of Livingston Island). The density parameter presented (σ) is an anomaly of potential density (ρ), defined by $\sigma = (\rho - 1) \times 10^3$ and explained by Lynn and Reid (1968). The anomalies σ_0 , σ_2 and σ_4 are calculated from potential densities relative to the sea surface, 2000 db and 4000 db and are used to characterize density above 1 km, between 1 and 3 km, and below 3 km.

The distributions of characteristics on section II give evidence of several expected, though notable, features. The low-salinity, highly oxygenated Antarctic Surface Waters contain a subsurface temperature minimum with extreme values below -1°C near the northern extent of these waters at a depth of ~ 100 m. The southernmost part of the Polar Frontal Zone is marked by a slight meridional gradient in surface temperature, characteristic of the summer season. From south to north within this Zone, the subsurface temperature minimum deepens, decreases in magnitude and finally disappears. Within the Polar Frontal Zone a subsurface maximum in oxygen and minimum in salinity are seen to extend from the surface layer downward to the north. This high-oxygen, low-salinity water is characteristic of Antarctic Intermediate Water.

The Circumpolar Deep Water (CDW) is seen to fill most of the Passage. It is characterized by low oxygen and relatively high salinity values, and south of the Polar Frontal Zone by a relative maximum in temperature. Throughout the Passage the high-salinity core lies beneath the extremum in dissolved-oxygen concentration.

Much of the coldest bottom water at the southern

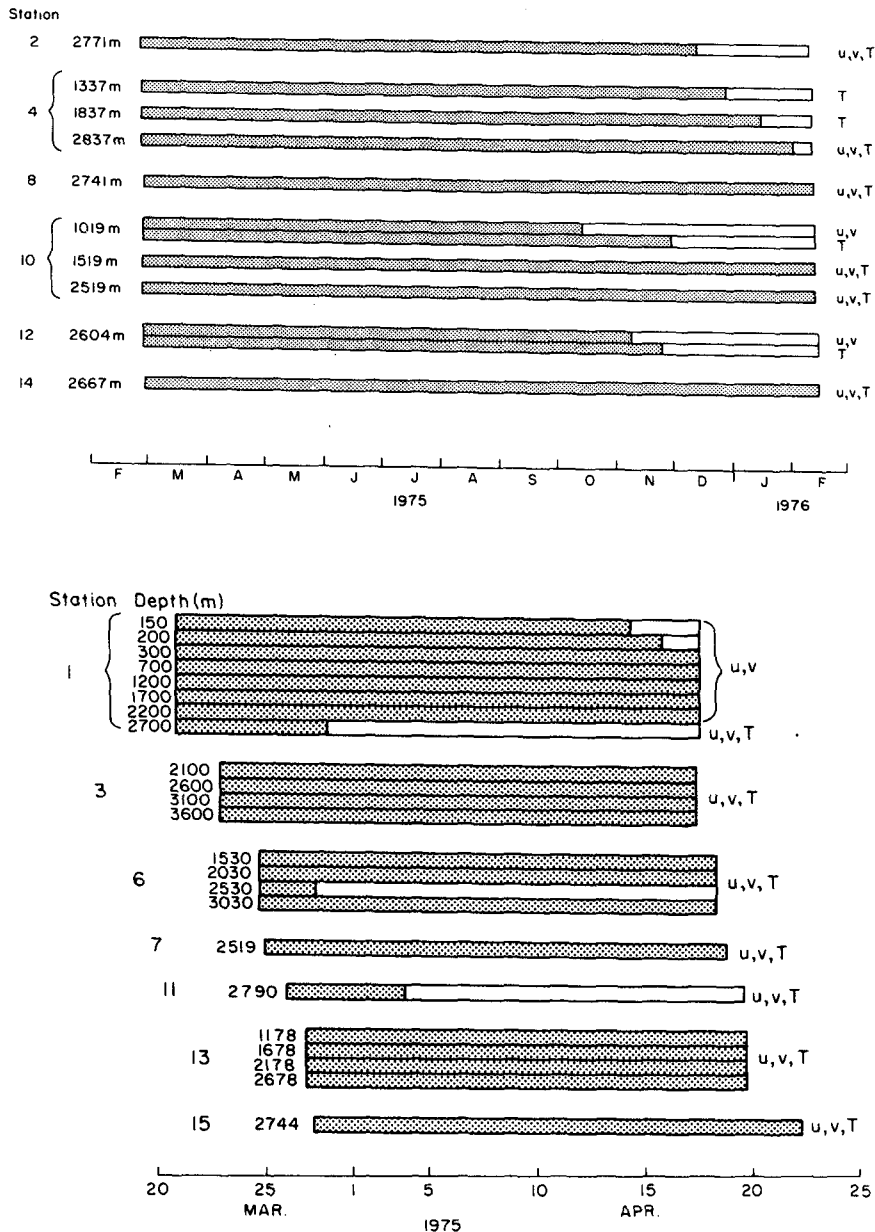


FIG. 3. Data return from current meter records.

end of the Passage lies within a trench, seen to extend almost to 4800 m in section II. Since this trench appears closed to the east and west of the section, free communication through the Passage of water with σ_4 greater than 46.1 is unlikely.

Most previously reported density sections across the Antarctic Circumpolar Current are based on stations spaced almost 100 km apart. The horizontal resolution resulting from the closely spaced stations on section II reveals vertically coherent bands of isopycnal slope somewhat steeper than the general downward slope of isopycnals toward the north. As contoured using station data with about 50 km horizontal separation,

the density field has a step-like appearance which seems to be vertically coherent.

The density structure observed on *Melville* section V (Fig. 5) also shows these bands. Section V differs from II in that it does not extend quite as far into shallow water at the northern end of the Passage. Also the two bands of relatively large horizontal density gradient seen near the center of the Passage in section II appear as only one band on section V—probably due to a different orientation of the current and water mass structure on the two different crossings.

Data from cruises of the *Ob* in 1958 (Eskin, 1959), the *Washington* in 1969 (Reid and Nowlin, 1971) and

the *Hudson* in 1970 (Foster, 1972) also provide some evidence for bands of relatively large horizontal density gradients (geostrophic shear) embedded in the current through Drake Passage. However, the station separations (at least 100 km) on these cruises were somewhat too large to enable unambiguous descriptions of the current structure.

In Fig. 6 is shown the density section made in March 1976 during FDRAKE 76, along a line parallel to and approximately 25 km east of the current meter

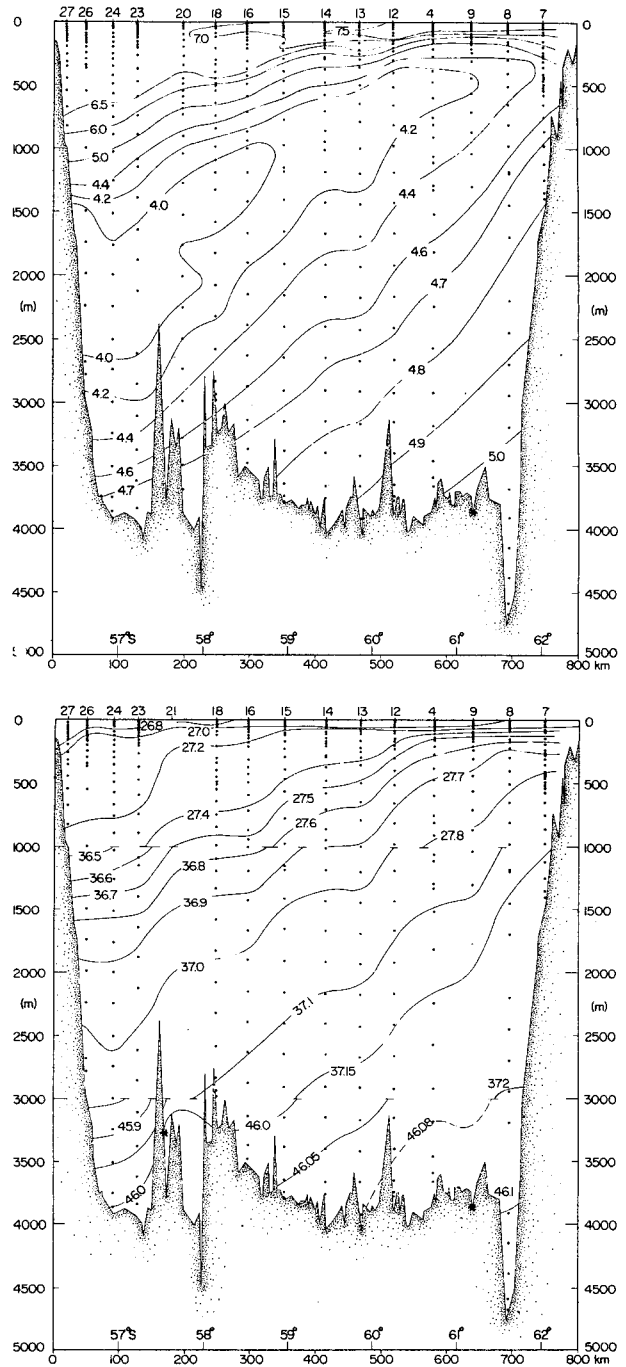
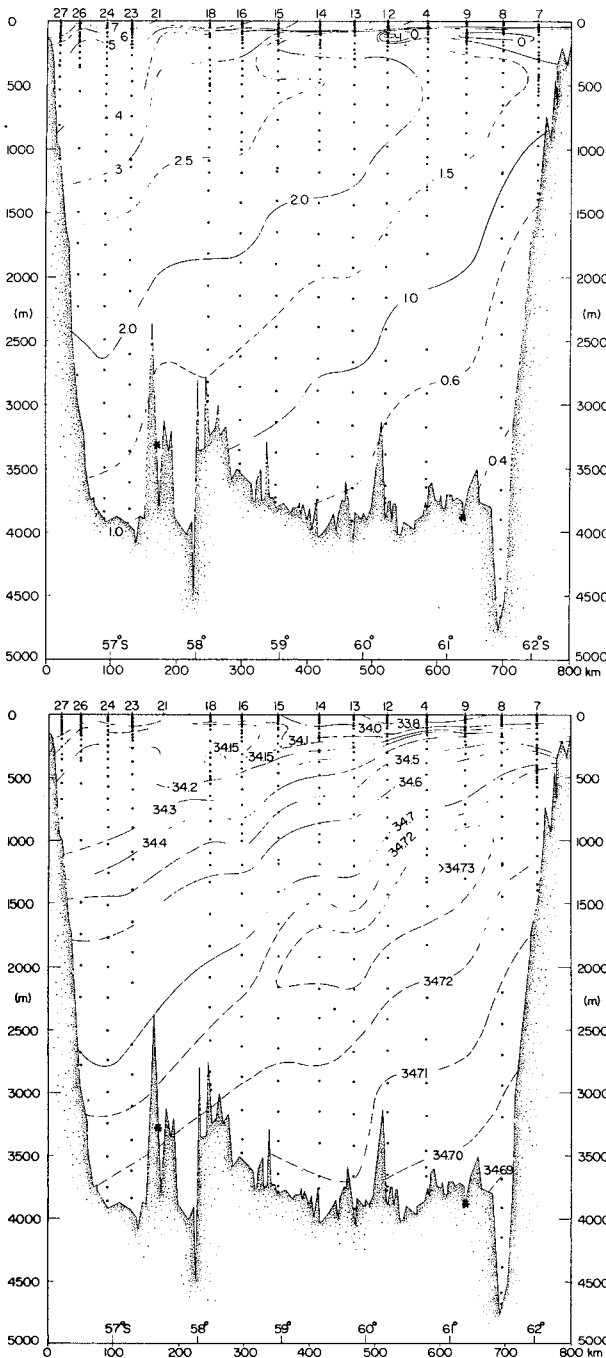


FIG. 4. *Melville* section II, FDRAKE 75, across Drake Passage: (a) temperature ($^{\circ}\text{C}$), (b) salinity (‰), (c) dissolved oxygen (ml l^{-1}), and (d) density parameter σ (kg m^{-3}). Dots indicate depths of bottle data. An asterisk marks deepest STD observations at stations 9 and 21.

array. On this section the station spacing was approximately 45 km. There are three bands of high horizontal density gradient, or cores of relatively strong flow, in this section.

The T - S traces from STD measurements made on

Melville section II are shown in Fig. 7. The common underlying CDW appears as a broad salinity maximum which is located near 2000 m in the northern Passage and near 500 m in the south (Fig. 4). The *T-S* relations for waters above the core of the CDW can be grouped into four distinct regimes. The boundaries between these surface water mass regimes correspond to the regions of large horizontal density gradient associated with the step-like rise of the CDW toward the south.

The stations north of the northernmost band of large horizontal density gradient (Fig. 7a) are representative of Pacific Subantarctic Surface Water (SASW). Mixing within the Pacific sector of the Southern Ocean produces a spatially homogeneous water mass characterized by a tight *T-S* relationship.

Stations within the Antarctic Surface Water (AASW) regime are presented in Fig. 7c. The traces are rather uniform in shape, although not as tight as the SASW regime, with a temperature minimum near 125 m. In Fig. 7b are shown *T-S* traces from stations within the Polar Frontal Zone (PFZ) which is seen to be a transition zone between the SASW and AASW regimes. The interleavings of these two water masses appear as reversals in the *T-S* curves, which occur just below the temperature minimum in the southern PFZ and reach depths of 500-800 m in the northern PFZ. This small scale variability makes the character of *T-S* relationships within the PFZ markedly different from those of the other water mass regimes.

The traces in Fig. 7d are from stations south of

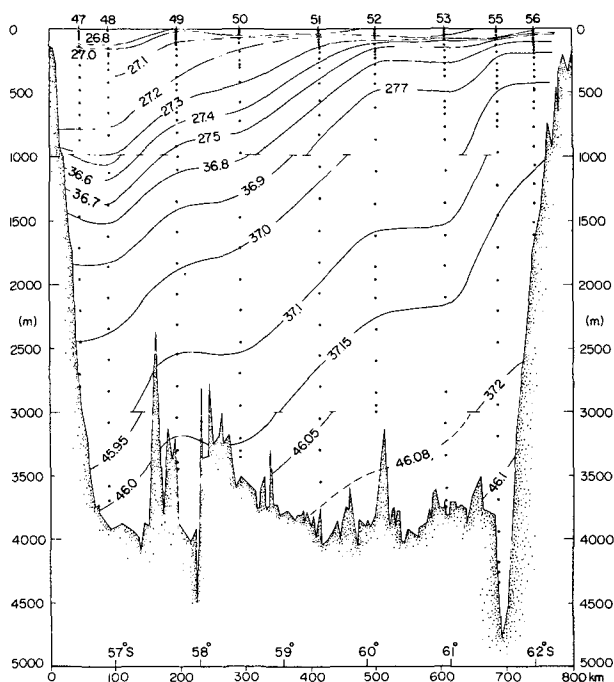


FIG. 5. Density parameter σ (kg m^{-3}) in *Melville* section V, FDRAKE 75, across Drake Passage.

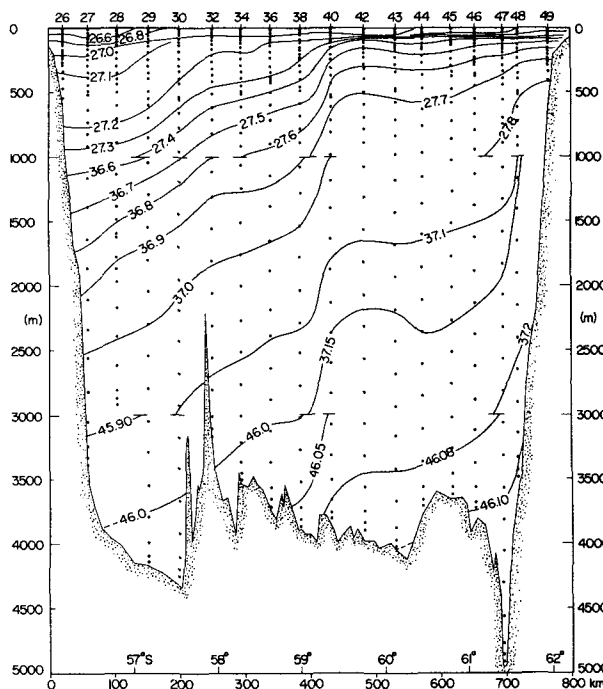


FIG. 6. Density parameter σ (kg m^{-3}) in *Thompson* section, FDRAKE 76, across Drake Passage.

the southernmost band of large horizontal density gradient. The waters of that regime, from the Bellingshausen Sea and Bransfield Strait, are found close to the South Shetland Islands and have a broad temperature minimum and a relatively sharp temperature maximum.

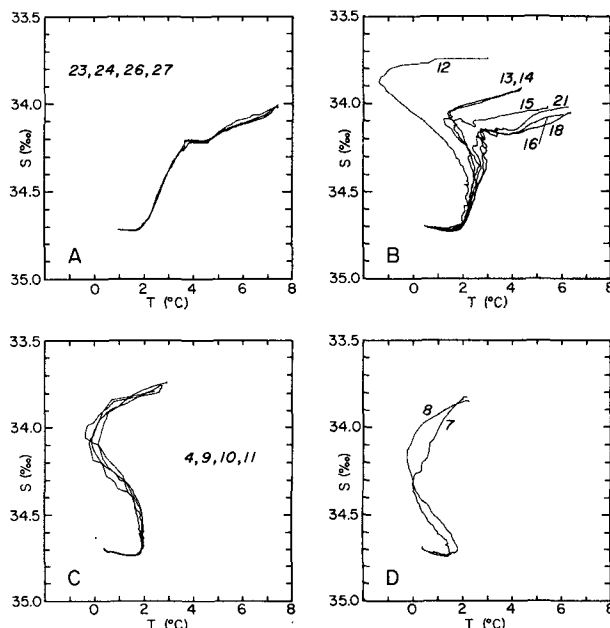


FIG. 7. *T-S* diagrams from *Melville* section II STD stations, FDRAKE 75.

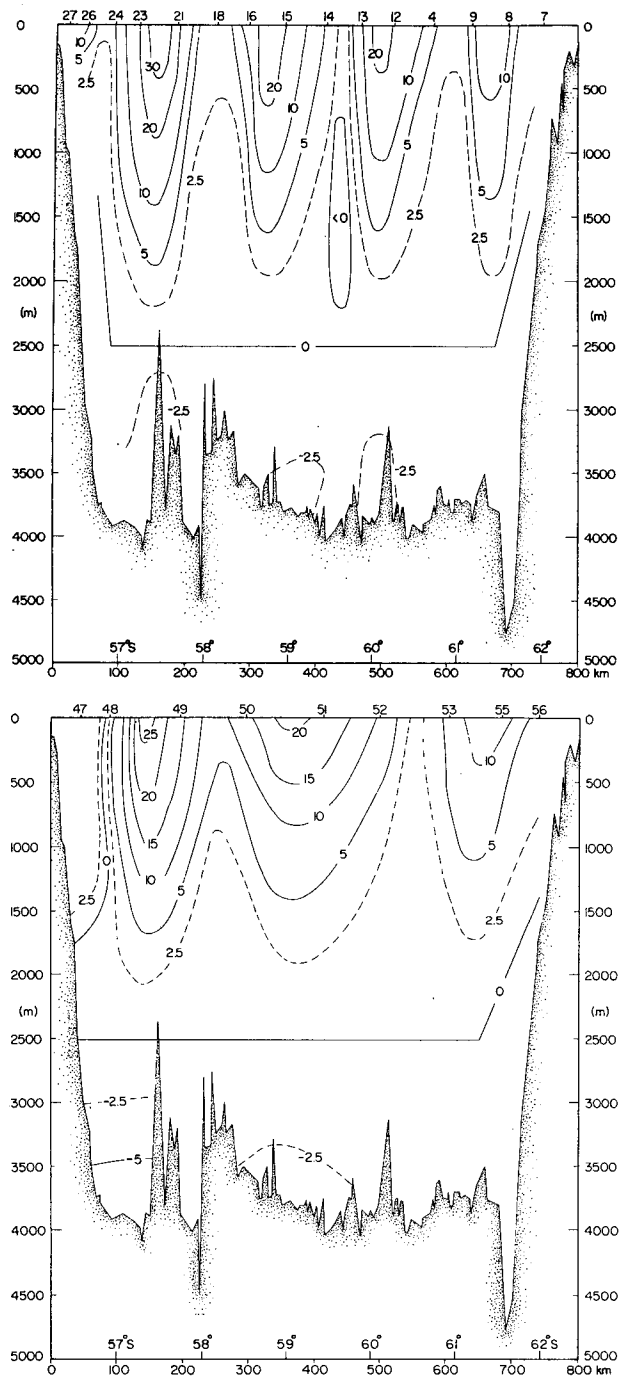


FIG. 8. Geostrophic speed (cm s^{-1}) relative to 2500 db normal to Melville sections II (a) and V (b), FDRAKE 75. Greatest common sample depth is used as reference for station pairs which did not reach 2500 db.

The T - S curves of stations in other FDRAKE sections can be similarly grouped into four distinct surface water masses, as can the hydrographic stations made by the *Ob* (Eskin, 1959) during the austral winter. These observations suggest that the zonation is a permanent feature of the ACC in Drake Passage.

4. Kinematic structure

a. Geostrophic velocity sections

Geostrophic speeds relative to 2500 db (or the greatest common sampling depth) were calculated for sections II and V (Figs. 8a and 8b). The general characteristics of the two sections are similar, showing bands of high eastward speeds separated by regions of lower speed or even westward flow in the central Passage. An eastward flow over the South American continental slope in section II does not appear in section V which ends at the 3000 m isobath. Temporal changes in the mass field and the greater horizontal resolution in section II result in the central high velocity core appearing as two bands.

b. Vertical shears

The positions of the current meter moorings and hydrographic stations were arranged to permit the adjustment of geostrophic speeds with directly measured speeds. Before any adjustment was made, however, the compatibility of these two different types of measurements was examined. The calculated geostrophic speed between two hydrographic stations represents the quasi-synoptic, spatially averaged baroclinic flow between the two stations. The current meters provide a time series of measurements of the baroclinic plus barotropic flow at a point fixed in space. To the extent that geostrophy holds in this region, the "absolute" speed (barotropic plus baroclinic) results when relative geostrophic speeds are referenced to the directly measured speed averaged over some time period. To determine the appropriate averaging period, moorings with more than one in-

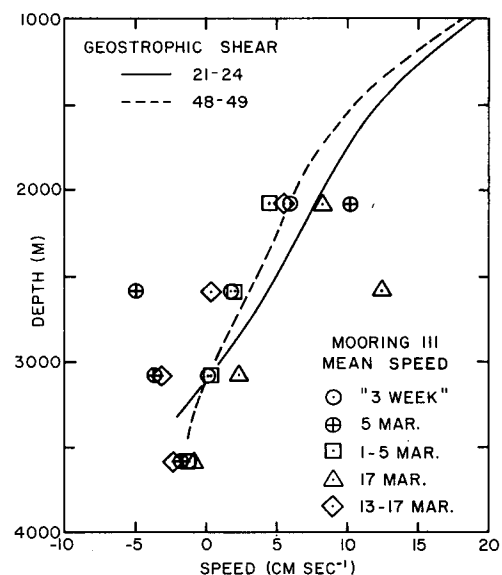


FIG. 9. Current shears from direct measurements at mooring III (averaged for different time periods) and geostrophic shears for stations 21-24 and 48-49, Melville FDRAKE 75.

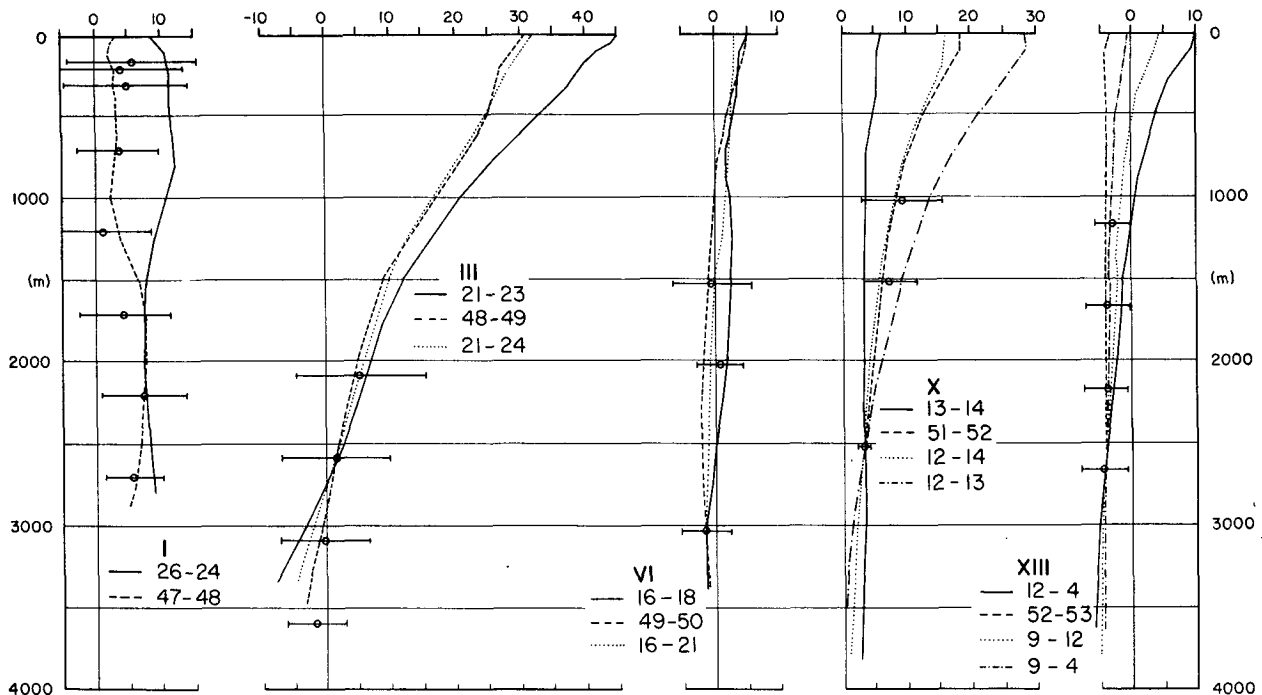


FIG. 10. For moorings having more than one current meter, comparison of directly-measured current shear, using three-week average velocities, with geostrophic shears calculated from *Melville* density sections II and V. Error bars show standard deviation of directly measured daily mean velocity.

strument were used to compare geostrophic and directly measured current shear.

Fig. 9 shows the geostrophic shears from two station pairs referenced to the "three-week" average speed of the current meter at 3081 m on mooring III. Also shown are the mean speeds recorded during the days that station pairs 21-24 (5 March) and 48-49 (17 March) were made and the 5-day means prior to these days. The two pairs of stations were located about the same distance apart and have similar geostrophic shears. The one-day averages were least representative of the shear calculated from the mass field; agreement between geostrophic shear calculated from the density measurements and shear from directly measured currents improves with increasing averaging periods.

For moorings with more than one current meter the shears from three-week current averages are compared with geostrophic shears from station pairs on sections II and V obtained at the beginning and end of the three-week period (Fig. 10). The geostrophic shears are referenced to the observed speed of the appropriate current meter closest to 2700 m. Some differences in the directly measured and calculated speeds are expected due to temporal changes in the mass field and different station separations which change the spatial average of geostrophic speeds. Both effects are illustrated in the comparisons at mooring X in Fig. 10. Stations 52 and 12 are nearly co-located as are stations 51 and 14. The relative

shears for the two pairs are almost identical, both showing good agreement with the directly measured shear. When an intermediate station from section II is used, we see that the geostrophic shear between stations 13 and 14 which span mooring X is not representative of the three-week mean current meter shear. (A 5-day average of shears from mooring X shows excellent agreement with station pair 13-14, however.) The high-velocity core found between stations 12 and 13 on section II apparently moved north prior to section V, raising the three-week average current meter speeds.

The other multiply-instrumented moorings shown in Fig. 10 show various degrees of agreement. In spite of the differences, it is encouraging to note that regions having large geostrophic shear coincide with moorings showing large shears.

c. Adjusted velocity sections

The geostrophic shear between stations on *Melville* section II was adjusted to the component of current meter velocity normal to the station pair. The current meter closest to 2700 m was used from moorings with more than one instrument. The adjustment was made using the mean velocities for the period of operation of the short-term meters (20-22 days) and the first 22 days recorded for the long-term meters. Fig. 11 shows the resulting section of adjusted speeds and gives the mooring numbers and the current meter

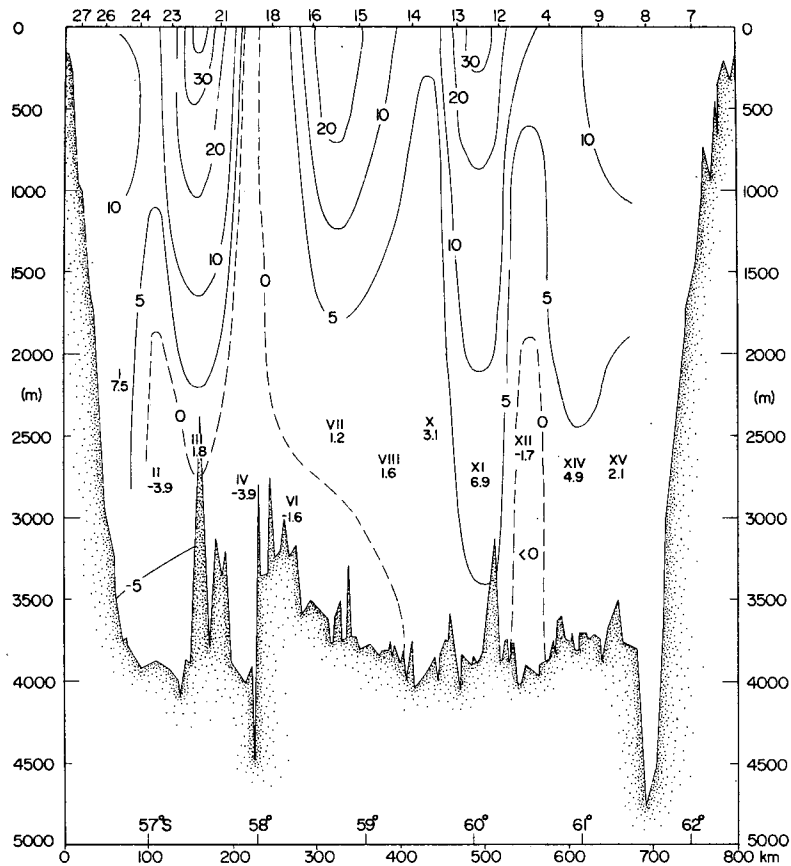


FIG. 11. Adjusted speed (cm s^{-1}) normal to *Melville* section II, F Drake 75. Reference speeds used from direct current measurements are shown.

speeds used in constructing the section. Moorings V (lost), IX (deployed after *Melville* section II was completed) and XIII (not bracketed by a pair of hydrographic stations) were not used in preparing this section of adjusted speed.

Comparison of Fig. 11 with Fig. 8a shows the changes in structure between the adjusted and the relative geostrophic speeds. The small adjustment from the meter on mooring X is enough to eliminate the relative counterflow (westward) between stations 13 and 14, while the westward flow at mooring IV results in a counterflow between stations 18 and 21. A small region of westward flow is still seen in the deeper layers of the northern half of the section. The adjustments to section V (not shown) resulted in essentially the same kinematic structure as that relative to 2500 db (Fig. 8b). Although small adjustments from current measurements result in only minor changes to the speed field, they have a significant effect on the adjusted transport.

5. Transport estimates

a. Relative geostrophic flow

Calculations of relative geostrophic transport through Drake Passage based on the F Drake data agree

quite well with calculations based on earlier measurements. The locations of the F Drake sections and five earlier sections are shown in Fig. 12 along with the estimates of geostrophic transport. As pointed out by Reid and Nowlin (1971), who compared geostrophic transports from the first four cruises shown in Fig. 12, the overall pressure field and thus the relative geostrophic transport is almost constant for the different measurement suites compared.

b. Adjusted transport estimates

Current meter records have been used to reference the relative geostrophic speeds calculated from density measurements. Then, the resulting section of speed normal to the current meter array can be integrated to obtain an adjusted transport estimate. When considering this approach, several questions arise.

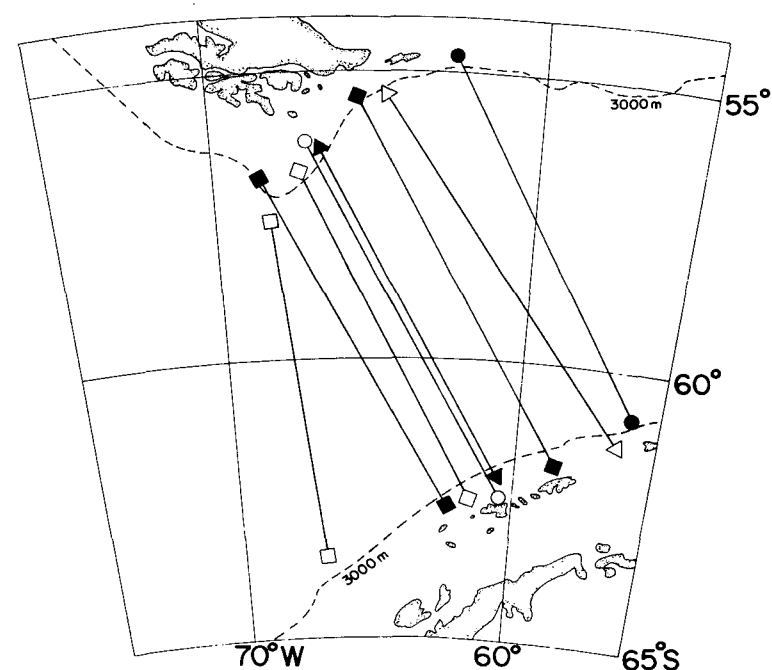
What length of current meter records should be used in obtaining average velocities for use in referencing the geostrophic calculations? Since we are seeking estimates of the net transport, we must certainly remove short-period tidal and inertial responses, which we feel we accomplished effectively by subjecting the records to a low-pass filter with a 40 h half-power point. We then considered the results of

our comparisons of directly measured vertical shear with calculated geostrophic shear. In most cases it was apparent that one- or two-day averages gave measured shears which differed significantly from the geostrophic shears as compared with averages of about one week. Moreover, averages over the entire period of the short-term array did not give shears significantly different from one-week averages, so it was decided to reference the geostrophic calculations with components of the measured velocity averaged over the entire short-term record lengths.

Since directly measured and geostrophic shears do not agree perfectly, from what levels should the measured currents be used to reference the geostrophic calculations? Rather than attempt what seemed to be arbitrary selections, we present the values resulting from all of the various possibilities.

How steady is the density field? We have attempted to answer this by repeating the calculations using two realizations of the density field: *Melville* section II, occupied just after the installation of the current meter array, and *Melville* section V, a repeat of section II made approximately three weeks later during the recovery of the short-term array.

How much variation might we expect between the resulting estimate of adjusted transport and another estimate made in the same manner but during a different three-week period? This includes not only the variability at periods greater than three weeks (which we hope to answer by a continuing program of monitoring) but also the question of how representative is a specific set of current measurements. What might one expect to obtain if the experiment were repeated many times? In the accompanying paper by Bryden



	VESSEL	EXPEDITION	DATE	TRANSPORT ($10^6 \text{ m}^3/\text{sec}$)
○—○	DISCOVERY II		April 1930	84
(Not Shown)	DISCOVERY II		March 1934	88 [†]
◁—▷	OB		June 1958	87
◇—◇	WASHINGTON	PIQUERO	Jan. 1969	103
□—□	HUDSON		Feb. 1970	75
◄—►	MELVILLE	FDRAKE 75 (II)	March 1975	111
■—■	MELVILLE	FDRAKE 75 (III)	March 1975	110
◆—◆	MELVILLE	FDRAKE 75 (IV)	March 1975	80
◄—►	MELVILLE	FDRAKE 75 (V)	March 1975	106
●—●	MELVILLE	FDRAKE 75 (VI)	March 1975	68
◄—►	THOMPSON	FDRAKE 76	March 1976	110

TRANSPORTS RELATIVE TO GREATEST COMMON SAMPLE DEPTHS HAVE BEEN INCLUDED WHEN STATIONS DID NOT REACH 3000 DB.
[†]SECTION ALONG 80°W.

FIG. 12. Geostrophic transport through Drake Passage above and relative to 3000 db.

TABLE 1. Adjusted transport through Drake Passage (*Melville* section II).

Station pair*	Greatest common depth (m)	Current measurements			Relative transport†		Adjusted transport Sum	Adjusted transport Average	
		Mooring	Depth	Mean speed**	Transport***	Above current meter			Below current meter
26-24 (40)	2778	I	150	5.9	6.6	-0.1	-2.1	4.4	4.6
			200	3.9	4.3	-0.1	-2.2	2.1	
			300	5.0	5.6	-0.1	-2.2	3.3	
			700	3.7	4.1	-0.2	-2.8	1.1	
			1200	1.2	1.3	1.0	-0.8	1.6	
			1700	4.5	5.0	2.0	0.2	7.2	
			2200	7.5	8.3	1.7	0.2	10.2	
	2700††	5.9	6.6	0.4	0	7.0			
24-23 (42)	3891	II	2771	-3.9	-6.4	7.8	-0.9	0.5	
23-21 (55)	3267	III	2081	5.8	10.6	18.4	-4.5	24.5	28.3
			2581	1.8	3.3	24.3	-1.9	25.7	
			3081	0.3	0.6	34.6	-0.5	34.7	
21-18 (57)	2975	IV	2837	-3.9	-6.6	1.4	0	-5.2	
18-16 (50)	2975	VI	1530	-0.4	-0.6	0.3	-1.2	-1.5	0.9
			2030	0.7	1.0	1.2	-0.7	1.5	
			3030	-1.6	-2.4	5.0†††	0	2.6	
16-15 (52)	3516	VII	2519	1.2	2.2	15.0	-0.7	16.5	
15-14 (64)	3769	VIII	2741	1.6	3.9	7.8	-1.0	10.7	
14-13 (54)	3794	X	1019	9.2	18.9	0.6	-0.1	19.3	13.9
			1519	7.2	14.8	0.5	0	15.2	
			2519	3.1	6.4	0.8	-0.1	7.1	
13-12 (47)	3773	XI	2790	6.9	12.2	13.0	-0.7	24.6	
12-4 (63)	3631	XII	2604	-1.7	-3.9	7.4	-0.6	2.9	
4-9 (61)	3631	XIV	2667	4.9	10.9	1.9	-0.1	12.7	
9-8 (52)	3926	XV	2744	2.1	4.3	9.4	-0.4	13.3	

* Separation in kilometers is shown in parentheses.

** Component normal to station pair, positive "eastward" (cm s^{-1}).

*** Station separation \times greatest common depth \times mean speed ($10^6 \text{ m}^3 \text{ s}^{-1}$).

† Geostrophic transport relative to current meter depth.

†† 6-day record.

††† Transport relative to 2975 m.

and Pillsbury, 7-day segments of year-long records have been examined and estimates have been made of the spatial distribution of variance in the currents near 2700 m and of the temporal variability of the spatially averaged current.

Between pairs of hydrographic stations on both sections II and V, we have used the current records from the short-term array to adjust the geostrophic speeds in order to estimate the volume transport normal to the station pairs. Table 1 presents the resulting estimates for station pairs on section II referenced separately for each current record obtained between the station pair. Analogous information based on section V is presented in Table 2.

The mean adjusted transport for section II is $124 \times 10^6 \text{ m}^3 \text{ s}^{-1}$ calculated using the average adjusted transport for the four moorings which had more than one current meter. If the largest and smallest transport values for these four moorings are used the transport ranges from 107 to $143 \times 10^6 \text{ m}^3 \text{ s}^{-1}$. The average standard deviation for the multi-instrumented moorings is $4.3 \times 10^6 \text{ m}^3 \text{ s}^{-1}$. If this variability is assumed for all 12 moorings and the variability in transport is distributed randomly east and west across each mooring the estimate of the range is from 109 to $139 \times 10^6 \text{ m}^3 \text{ s}^{-1}$ [$124 \pm 4.3(12^{\frac{1}{2}})$]. The transport adjusted to the current meters nearest 2700 m on each mooring is $122 \times 10^6 \text{ m}^3 \text{ s}^{-1}$.

The short-term current measurements were also used to adjust geostrophic transports calculated for *Melville* section V. There were only eight hydrographic stations on this section, but current measurements from 13 moorings are available for referencing the transports. Two moorings were located between each station pair except the most southern pair. For these pairs the transports adjusted to both current meters are presented in Table 2. The averaged values are also presented for multiply-instrumented moorings. Averaging the values when two moorings are located between a stations pair yields an adjusted transport estimate of $110 \times 10^6 \text{ m}^3 \text{ s}^{-1}$. The average standard deviation of adjusted transports using the five multiply-instrumented moorings and density from section V is $2.6 \times 10^6 \text{ m}^3 \text{ s}^{-1}$. Using section V and the average current values nearest 2700 m gives an adjusted transport of $104 \times 10^6 \text{ m}^3 \text{ s}^{-1}$.

As mentioned, previous direct current measurements have been made in Drake Passage. However, only two attempts have resulted in enough successful measurements, together with density measurements, to warrant presenting transport estimates. These are the estimates of $237 \times 10^6 \text{ m}^3 \text{ s}^{-1}$ eastward by Reid and Nowlin (1971) and $15 \times 10^6 \text{ m}^3 \text{ s}^{-1}$ westward by Foster (1972). These values differ greatly from one another and also from the present estimates. Reid and Nowlin's estimate is supported by the work of Callahan (1971) who used the same technique at 132°E between Australia and Antarctica. Referencing geostrophic velocities to one- or two-day records from five deep current meters he calculated an absolute transport of $233 \times 10^6 \text{ m}^3 \text{ s}^{-1}$ east. In spite of the short duration of his direct measurements and the large distances ($\sim 700 \text{ km}$) between current meters there is a remarkable agreement between Callahan's measurement of in-

 TABLE 2. As in Table 1 except for *Melville* Section V.

Station pair*	Greatest common depth (m)	Current measurements			Relative transport†		Adjusted transport Sum	Adjusted transport Average	
		Mooring	Depth	Mean speed**	Transport***	Above current meter			Below current meter
47-48 (37)	2865	I	150	6.2	6.6	0	2.8	9.3	5.8
			200	4.4	4.7	0	2.4	7.0	
			300	5.2	5.5	0	2.2	7.7	
			700	3.9	4.1	0	2.1	6.2	
			1200	1.2	1.3	-0.3	2.1	3.1	
			1700	4.4	4.7	-2.4	-0.2	2.1	
			2200	7.6	8.1	-2.3	-0.2	5.5	
	2700††	6.0	6.4	-1.1	0	5.2			
48-49 (107)	3453	II	2771	-3.5	-12.9	37.0	-1.3	22.8	41.1
			2081	5.8	21.4	26.6	-5.7	42.3	
		III	2581	1.8	6.7	33.6	-2.3	38.0	
			3081	0.2	0.7	42.7	-0.3	43.1	
49-50 (97)	3365	IV	2837	-3.7	-12.1	4.4	0.1	-7.5	2.4
			1530	-0.4	-1.3	3.7	-1.0	1.3	
		VI	2030	0.7	2.3	5.0	0.2	7.4	
			3030	-1.6	-5.2	3.7	0	-1.5	
50-51 (115)	3365	VII	2519	1.2	4.6	23.1	-1.4	26.3	
		VIII	2741	1.5	5.8	25.6	-0.8	30.6	
51-52 (92)	3013	X	1019	9.2	25.5	4.4	-6.3	23.6	22.5
			1519	7.1	19.7	6.8	-2.9	23.7	
			2519	3.1	8.6	12.0	-0.2	20.4	
		XI	2790	6.4	17.8	13.7	-0.1	31.4	
52-53 (94)	3013	XII	2604	-1.0	-2.8	0.5	0	-2.4	-10.6
			1178	-2.9	-8.2	0.1	-0.5	-8.6	
		XIII	1678	-4.0	-11.3	0.3	-0.3	-11.3	
			2178	-4.0	-11.3	0.7	0	-10.7	
			2678	-4.4	-12.5	0.8	0	-11.7	
53-55 (97)	3764	XIV	2667	4.9	17.9	13.9	-0.8	31.0	
		XV	2744	1.9	6.9	14.3	-0.6	20.6	

* Separation in kilometers is shown in parentheses.

** Component normal to station pair, positive "eastward" (cm s^{-1}).

*** Station separation \times greatest common depth \times mean speed ($10^6 \text{ m}^3 \text{ s}^{-1}$).

† Geostrophic transport relative to current meter depth.

†† Six-day record.

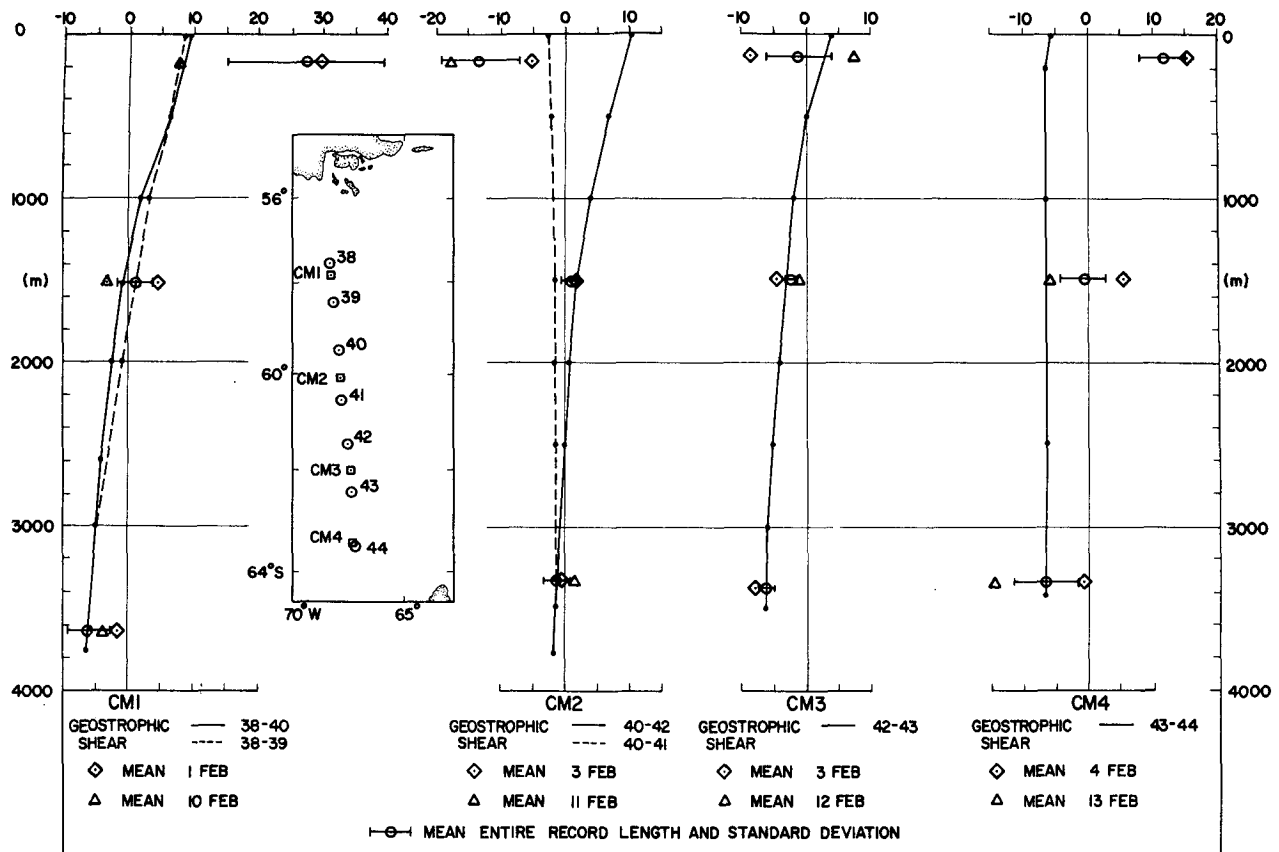


FIG. 13. Current shears from direct measurements and geostrophic shears for station pairs bracketing current meter arrays, *Hudson* 1970. Measured current components normal to station pairs are shown for the first and last day of measurement, and the entire record length. Standard deviation of daily means for record length are shown. Insert shows relative locations of stations and current meter moorings (after Foster, 1972).

flow into the Pacific and Reid and Nowlin's measurement of the Pacific outflow.

It was seen in the previous sections that the density field observed by Reid and Nowlin aboard the *Washington* is similar in both internal structure and in resulting relative geostrophic transport to that observed during FDRAKE. Moreover, the density section observed by Mann and Foster aboard the *Hudson* is also in reasonably close agreement with the FDRAKE relative transport estimates allowing for the fact that no stations were made in water depths of less than 3000 m at either end of the Passage.

The technique which we have used for adjusting our geostrophic transports is the same as that used by Reid and Nowlin (1971) with one exception. Reid and Nowlin had nine hydrographic stations across the Passage but only five current measurements, one of which was colocated with a hydrographic station. The current measurements were horizontally interpolated or extrapolated in order to reference the transport values between pairs of stations which did not bracket a current meter. In view of the banded nature of

the ACC in Drake Passage, this procedure may lead to significant errors.

Another possible reason for the large difference between our transport estimates and those of Reid and Nowlin is the very short length of their current measurements. Three of their records were of one-day duration and the other two were of three- and four-day duration. Our records show considerable variation in the daily mean speed and directions.

Using measurements made by Mann and Foster from the *Hudson* in 1970, Foster (1972) estimated the transport through Drake Passage using only their direct current measurements. Based on records of approximately 10-day duration from three meters on each of four moorings distributed across the Passage, he interpolated and contoured the measured speeds and calculated a transport of $15 \times 10^6 \text{ m}^3 \text{ s}^{-1}$ to the west. In view of the spatial variability we have observed in the density structure, it seems unlikely that four moorings are enough to adequately describe the speed distribution of the ACC within Drake Passage. Moreover, that the resulting transport estimate was westward rather than eastward can probably be ex-

plained by the circumstance, as noted by Foster, that the *Hudson* current meter moorings do not appear to have been located in regions of greatest baroclinic shear, i.e., in the bands of major eastward flow.

We have reexamined the *Hudson* data in order to make direct comparisons with the results of our FDRAKE measurements. The components of observed current meter speed normal to pairs of bracketing hydrographic stations are compared in Fig. 13 with the geostrophic shears for each station pair. (The positions of the *Hudson* current meter moorings and the hydrographic stations used are shown in the insert.) The geostrophic shears are referenced to the mean speed over the entire record length of the current meter closest to 3400 m. Also shown are the record length mean and standard deviation and the one-day means for the first day of operation of the meters and for the last day, recorded just before the hydrographic stations were occupied.

The observed and relative geostrophic shears show fair agreement between 1500 and 3400 m for moorings 1, 2 and 3 with poor agreement between these levels and 150 m, perhaps due to ageostrophic effects. The worst overall agreement is for the southernmost mooring which is located at about the latitude of station 44 and therefore not well bracketed by the station pair 43-44.

Station pairs 38-40, 40-42, 42-43 and 43-44 were selected to adjust the geostrophic transports to observed normal current components averaged over the largest integral number of days of record. The large differences between measured and calculated current shears are reflected in the adjusted transports relative to different meters which are summarized in Table 3. The adjusted transport estimates between individual station pairs differ as much as $193 \times 10^6 \text{ m}^3 \text{ s}^{-1}$, depending on the current meter used to reference the geostrophic speed. The adjusted transports for the entire section differ by only $38 \times 10^6 \text{ m}^3 \text{ s}^{-1}$ or about half the geostrophic transports relative to 3000 m.

6. Summary

In this paper we have described briefly some of the descriptive features of the Antarctic Circumpolar Current which might form the basis of theoretical/numerical studies. We have presented property distributions in vertical sections across Drake Passage. The density sections, which are based on station separations of ~ 50 km, show the Antarctic Circumpolar Current to consist of several bands of relatively large horizontal density gradients which are vertically coherent. These bands were present in sections separated by a three-week period during 1975 and were present again in 1976. They are likely permanent features of the Current regime, at least in Drake Passage. Three-week averages of direct current measurements from 13 moorings across the Passage were

TABLE 3. Adjusted transport through Drake Passage using *Hudson* 1970 data.

Hydrographic station pair	Eastward transport ($10^6 \text{ m}^3 \text{ s}^{-1}$) adjusted to current measurement at nominal depth of		
	150 m	1500 m	3400 m
38-40	147	15	-5
40-42	-177	7	16
42-43	-27	-8	-11
43-44	44	-3	-26
Σ	-13	11	-26

used to reference the relative geostrophic flow calculated from the density sections. The resulting adjusted speed field also shows kinematic banding with maximum eastward speeds of 25-30 cm s^{-1} in cores separated by eastward speeds of less than 5 cm s^{-1} or slight westward flow. The adjusted speeds were used to obtain an estimate of the volume transport through Drake Passage for March 1975 of $124 \times 10^6 \text{ m}^3 \text{ s}^{-1}$ to the east.

For moorings on which there was more than one current meter, the adjusted transport between the hydrographic station pair bracketing the mooring depends upon the current meter record used to reference the geostrophic calculations. This is because the directly observed shears and the geostrophic shears calculated from the density measurements do not exactly agree. One-day mean currents showed poor agreement with geostrophic shears, but agreement improved with increased averaging periods.

Based on three-week current averages, the variation of adjusted transport between stations pairs was examined for stations bracketing the multiply-instrumented current meter moorings. The standard deviation of the adjusted transport estimates was obtained for each such station pair and mooring. Averaging these standard deviations gives $3.8 \times 10^6 \text{ m}^3 \text{ s}^{-1}$ for one density section and $2.6 \times 10^6 \text{ m}^3 \text{ s}^{-1}$ for the other. This is a measure of the variation in transport due to the disparity between measured and geostrophic shears. The resulting range of transport for our most closely sampled density section is 110 to $138 \times 10^6 \text{ m}^3 \text{ s}^{-1}$.

Two other attempts were previously made to estimate the transport through Drake Passage using direct current measurements. These estimates were $237 \times 10^6 \text{ m}^3 \text{ s}^{-1}$ eastward by Reid and Nowlin (1971) and $15 \times 10^6 \text{ m}^3 \text{ s}^{-1}$ westward by Foster (1972). The technique used by Reid and Nowlin was the same as used here; the estimate of Foster was from direct current measurements alone. We have applied our technique to the density and current measurements of Foster. The disparity between our estimate and the previous estimates is discussed, and to some extent, explained.

Bryden and Pillsbury (1977) have estimated the

likely range of ACC transport estimates expected when referencing geostrophic calculations to deep current measurements over a one-week period. Their estimates, based on one-year records from six meters across Drake Passage, give a probable transport range of $262 \times 10^6 \text{ m}^3 \text{ s}^{-1}$. Extremes may occur over a longer observation interval and thus broaden this range. We would note that our estimate may be somewhat better than this range indicates, however, since we use three-week records from 13 moorings.

Acknowledgments. The United States component of the International Southern Ocean Studies is sponsored by the Office of the International Decade of Ocean Exploration, National Science Foundation. Ship support for the R/V *Melville* and the R/V *Thompson* during FDRAKE were provided by the Office of Oceanographic Facilities and Ships of the National Science Foundation. We wish to thank members of the Oregon State University current meter group, who under the field direction of Robert Still are responsible for the success of the moored array program during FDRAKE. The hydrographic station program aboard *Melville* during 1975 and *Thompson* during 1976 was directed by George C. Anderson to whom we are very appreciative.

REFERENCES

- Bryden, H. L., and R. D. Pillsbury, 1977: Variability of deep flow in the Drake Passage from year-long current measurements, *J. Phys. Oceanogr.*, **7**, 803-810.
- Callahan, J. E., 1971: Velocity structure and flux of the Antarctic Circumpolar Current south of Australia. *J. Geophys. Res.*, **76**, 5859-5864.
- Eskin, L. I., 1959: Contribution to the study of the water and thermal balance of Drake Passage (in Russian). [English translation: *Sov. Antarct. Exped. Inf. Bull.*, **2**, 52-55, Elsevier, Amsterdam, 1964].
- Foster, L. A., 1972: Current measurements in the Drake Passage. M.S. thesis, Dalhousie University, 61 pp.
- Lynn, R. J., and J. L. Reid, 1968: Characteristics and circulation of deep and abyssal waters. *Deep-Sea Res.*, **15**, 577-598.
- Nowlin, W. D., Jr., T. Whitworth III, L. I. Gordon and G. C. Anderson, 1977: Oceanographic Station Data collected aboard R/V *Melville* during FDRAKE 75. Data Rep., 77-2-D, Dept. of Oceanography, Texas A&M University, 355 pp.
- Pillsbury, R. D., J. S. Bottero, R. E. Still and W. E. Gilbert, 1974: A compilation of observations from moored current meters. Vol. 6, Oceanography of the Continental Shelf April-August 1972, Oregon State University Data Rep. 57, Ref. 74-2.
- , — and —, 1976: A compilation of observations from moored current meters. Vol. 9, Currents, temperature and pressure in the Drake Passage during FDRAKE 75, January-March 1975. Oregon State University Data Rep. 65, Ref. 76-6.
- Reid, J. L., and W. D. Nowlin, Jr., 1971: Transport of water through the Drake Passage. *Deep-Sea Res.*, **18**, 51-64.